

Altered structural networks and executive deficits in traumatic brain injury patients

K. Caeyenberghs · A. Leemans · I. Leunissen ·
J. Gooijers · K. Michiels · S. Sunaert · S. P. Swinnen

Received: 1 August 2012 / Accepted: 24 November 2012 / Published online: 12 December 2012
© Springer-Verlag Berlin Heidelberg 2012

Abstract Recent research on traumatic brain injury (TBI) has shown that impairments in cognitive and executive control functions are accompanied by a disrupted neural connectivity characterized by white matter damage. We constructed binary and weighted brain structural networks in 21 patients with chronic TBI and 17 healthy young adults utilizing diffusion tensor tractography and calculated topological properties of the networks using a graph theoretical method. Executive function was assessed with the local global task and the trail making task, requiring inhibition, updating, and switching. The results revealed that TBI patients were less successful than controls on the executive tasks, as shown by the higher reaction times, higher switch costs, and lower accuracy rates. Moreover, both TBI patients and controls exhibited a small world topology in their white

matter networks. More importantly, the TBI patients demonstrated increased shortest path length and decreased global efficiency of the structural network. These findings suggest that TBI patients have a weaker globally integrated structural brain network, resulting in a limited capacity to integrate information across brain regions. Furthermore, we showed that the white matter networks of both groups contained highly connected hub regions that were predominately located in the parietal cortex, frontal cortex, and basal ganglia. Finally, we showed significant correlations between switching performance and network property metrics within the TBI group. Specifically, lower scores on the switching tasks corresponded to a lower global efficiency. We conclude that analyzing the structural brain network connectivity provides new insights into understanding cognitive control changes following brain injury.

K. Caeyenberghs · I. Leunissen · J. Gooijers · S. P. Swinnen
Movement Control and Neuroplasticity Research Group,
Department of Kinesiology, Biomedical Sciences Group,
K.U.Leuven, Leuven, Belgium

K. Caeyenberghs (✉)
Department of Physical Therapy and Motor Rehabilitation,
Faculty of Medicine and Health sciences, University of Ghent,
De Pintelaan 185, 9000 Gent, Belgium
e-mail: Karen.Caeyenberghs@UGent.be

A. Leemans
Image Sciences Institute, University Medical Center Utrecht,
Utrecht, The Netherlands

K. Michiels
Department of Physical Medicine and Rehabilitation, University
Hospital, Leuven Campus Pellenberg, Leuven, Belgium

S. Sunaert
Radiology, Department of Imaging and Pathology,
Biomedical Sciences Group, K.U.Leuven, Leuven, Belgium

Keywords Diffusion tensor imaging · Graph theoretical analysis · Executive functioning · Structural network · Traumatic brain injury

Abbreviations

DAI Diffuse axonal injury
DTI Diffusion tensor imaging
FA Fractional anisotropy
LGL Local global task
TBI Traumatic brain injury
TMT Trail making task
WM White matter

Introduction

Traumatic brain injury (TBI) is a non-degenerative, non-congenital insult to the brain from an external mechanical

force, possibly leading to permanent or temporary impairment of cognitive, physical, and psychosocial functions, with an associated diminished or altered state of consciousness (Timmons 2012). TBI can result from multiple causes, including motor vehicle accidents, bicycle accidents, falls, and sport injuries. TBI is a major cause of death and disability worldwide, especially in children and young adults (Kraus and McArthur 1996; Sosin et al. 1996), demanding early and accurate diagnosis, assessment of severity, and prognostication of likely outcomes. Specifically, each year, TBI contributes to a substantial number of deaths (an average mortality of about 15 per 100,000 in Europe) and a high number cases of permanent disability (an incidence rate of about 235 per 100,000 in Europe) (Bruns and Hauser 2003; Maas et al. 2008; Tagliaferri et al. 2006). Hence, the burden on public health and social care is substantial (Thurman et al. 1999). Neurobehavioural deficits associated with cognition are often the cause of significant disability after TBI. Observed cognitive changes that follow TBI, even years after injury, can include decreased mental flexibility, trouble shifting sets, impaired attention, poor planning, lack of organization, problems with sequencing, impaired judgment, deficits in verbal fluency, problems with working memory, as well as increased impulsivity (Levin and Kraus 1994; Godefroy 2003). These persistent dysfunctions arise from diffuse axonal injury (DAI), which damages the integrity of the white matter (WM) tracts that connect brain regions.

Diffusion tensor imaging (DTI) provides a validated and sensitive way of identifying the impact of DAI (Levin 2003). The relationship between cognitive impairment after TBI and white matter damage has been established in previous studies, such that greater white matter pathology predicts greater cognitive deficits (Kinnunen et al. 2011; Kraus et al. 2007; Niogi et al. 2008a, b; Kennedy et al. 2009). However, these studies have typically focused on a limited number of brain locations defined by regions of interest, such as the superior longitudinal fasciculus, corpus callosum, cingulum fibre bundles etc. (Kraus et al. 2007; Niogi et al. 2008a, b; Kennedy et al. 2009). This approach is a sensitive way of identifying white matter damage, but it is restricted to assessment of a priori defined regions. Accordingly, only a small amount of the total white matter is usually investigated. Moreover, as executive control depend on the coherent activity of widely distributed networks, such an approach limits analysis of the structural causes of cognitive deficits. Network-based measures of structural connectivity can be more sensitive to alterations that are less apparent in gross structure (i.e., WM integrity) because they consider each region's integration into the global unit rather than as an independent entity. Thus, to obtain novel information about neural communication pathways, it is also important to explore the characteristics of the brain network in TBI patients.

Recent studies have suggested that the human white matter network, reconstructed with diffusion MRI tractography, can be characterized quantitatively with a graph theoretical analysis (for reviews, see Bullmore and Sporns 2009). However, apart from two recent DTI network studies, one on healthy young adults (17–33 years) (Li et al. 2009) and the other on elderly people (72–92 years) (Wen et al. 2011), no study currently exists in which DTI network properties have been related to cognitive functions in TBI adults. In the present study, we used DTI-based fiber tractography to reconstruct the human brain WM networks of 21 TBI and 17 control participants, followed by a graph theoretical analysis. Given widespread impaired connections previously reported in TBI, we hypothesized that patients with TBI would show a decreased structural connectivity in the white matter networks.

In particular, we examined correlations of brain (sub) cortical structural connectivity with executive function performance. Two executive control tasks were applied, one based on the empirical constructs and the other one on more clinical measures. The first task, the local global task (LGT), has been used as a research tool to investigate the ability to suppress attention to the more salient aspects of perceptual displays (Navon 1977). The second one, the trail making task (TMT), is a neuropsychological test that involves motor speed and attentional control and is used diagnostically as a test of frontal lobe functioning (e.g., Demakis 2004; Gouveia et al. 2007). To use the set of executive control components identified by Miyake et al. (2000), both tasks require inhibition (ignore misleading cues), updating (monitor display in the context of current instructions), and switching (adjusting response according to current rule). Moreover, in both tasks, the presence of conflict creates conditions in which the executive demands can be increased (switch trials) or reduced (repeat trials).

We hypothesized that (1) patients with TBI would perform more poorly than controls on the switch trials, and that (2) these executive control deficits would correlate with decreases in structural connectivity, underscoring the functional significance of the connectivity metrics.

Materials and methods

Participants

Thirty-eight adults participated in the study, including 21 patients with moderate to severe TBI (mean age = 25 years 6 months; SD = 5 years 4 months; 15 males and 6 females), who had sustained closed head trauma due to traffic accident or sport injury that averaged 4 years 3 months before the study (SD = 2 years 5 months), and 17 control subjects (mean age = 25 years; SD = 1 year

8 months; 8 males and 9 females). The TBI patients were classified according to the Mayo Classification System for traumatic brain injury severity as ‘moderate-to-severe’ based on the several factors: the post resuscitation Glasgow Coma Scale (Teasdale and Jennett 1974) (only available from four patients, $M = 7.8$, range = 4–12), the duration of loss of consciousness (30 min or more), the length of post-traumatic amnesia (>1 day), the anatomical features of the injury based on the inspection by an expert neuro-radiologist (see below), and the injury mechanism (traffic accidents and falls), or combinations thereof. Exclusion criteria were as follows: neurosurgery, except for invasive intracranial pressure monitoring; a history of psychiatric or neurological illness prior to the head injury; a history of previous traumatic brain injury; anti-epileptic medication; current or previous drug or alcohol abuse; or contraindication to MRI.

The structural MRI scans (see below) were inspected and classified by an experienced neuro-radiologist (S.S.) using the scheme of Adams et al. (1989), which allows the identification of three grades of diffuse axonal injury (see Table 1). In grade 1, there is evidence of axonal injury in the white matter of the cerebral hemispheres, the corpus callosum, the brainstem and, less commonly, the cerebellum; in grade 2, there is also a focal lesion in the corpus callosum; and in grade 3 there is also a focal lesion in the dorsolateral quadrant or quadrants of the rostral brain stem. The median severity score of the TBI patients was 2 (range = 0–2.5). Demographic and neurologic variables are provided in Table 1. The 17 control subjects had normal medical histories and MRI scans were rated as being “normal” by a radiologist. All subjects were right handed (laterality quotient: TBI: mean = 81, range = 22–100; control: mean = 92; range = 60–100) as verified by the Edinburgh Handedness Inventory (Oldfield 1971). The study was approved by the local ethics committee for biomedical research. Informed consent was obtained from each patient or from the patient’s first-degree relatives.

Behavioral testing

Assessment of executive function was performed using two tasks, one based on the empirical constructs, i.e. the LGT, and the other used in more clinical applications, i.e. the TMT.

Local global task (LGT)

Participants performed the LGT (derived from Miyake et al. 2000) with their right hand. The target stimulus (as shown in Fig. 1) consisted of a “global” square or rectangle, composed of much smaller “local” squares or rectangles. Each trial began with the presentation of a

prime cue, indicating to which dimension to attend. The global dimension was cued by a big square, to the left of the stimulus, and a big rectangle to the right. For the local dimension, the same square and rectangle appeared, only smaller. After a random cue-target interval of 400–600 ms, the target stimulus was presented. Both the cue and the target stimulus remained on the screen until a participant responded, or until 2,500 ms had elapsed. Participants were required to identify the relevant target stimulus dimension and press one key with their index finger for squares and another with their middle finger for rectangles (Fig. 1). The interval between a response and the presentation of the next trial varied randomly between 900 and 1,100 ms. The experiment comprised two unidimensional blocks, and one switch block. In the unidimensional blocks, participants attended to either the global cues or the local cues. The order was counterbalanced across participants. In the third switch block, the target stimulus dimension alternated every other trial (i.e., two “local” trials, followed by two “global” trials, etc.). When the prime cues changed, the participants had to switch from responding to the local dimension to the global dimensions of the target stimulus, and vice versa. A short amount of practice was given to ensure the instructions were understood (four trials for each unidimensional block, and 8–16 trials for the switch block). The experiment consisted of 24 trials in each pure block, and 49 trials in the switch block. Variables of interest were RT and accuracy on repetition trials and on switch trials, and switch cost (=RT switch trial – RT repetition trial). The whole task took about 15 min.

Trail making task (TMT)

The TMT has been extensively researched and has demonstrated its usefulness for assessing cognitive compromise in a variety of clinical populations. The TMT is also well established as a sensitive measure of cognitive problems associated with traumatic brain injury (e.g., Axelrod et al. 2001; Guilmette et al. 1999; Stuss et al. 2001). This neuropsychological test consists of two parts, Trails A and Trails B. In Trails A, letters from A to Y are distributed across the page and participants are asked to draw lines connecting the letters from the alphabet in the right order, without lifting the pencil from the page. In Trails B, the page contains the numbers from 1 to 12 and letters from A to L and participants must connect the symbols by alternating the sequence between numbers and letters, that is, A-1-B-2-C-3...L-12. The experimenter explained each task and participants completed a practice version containing fewer items. The dependent variables were the time to complete Parts A (connecting letters from the alphabet in the right order) and B (connecting numbers and letters in sequential order) separately, plus a switch cost calculated

Table 1 Summary of demographic and injury characteristics for the TBI group. Anatomy codes

TBI patient age/ gender	Age at injury	GCS score	Acute scan within 24 h after injury Lesion location/pathology	MRI scan at examination Lesion location/pathology	Severity score
TBI 1 27.6/F/RH	25.2	12	TL contusion, (R) PL haemorrhage, (L) FL intraparenchymateus haemorrhagic contusion, subdural haematoma	Drain tract (R), (L) FL and TL contusion	2
TBI 2 22.9/F/RH	21.3		(R) FL haemorrhage, (L) FL/TL and (L) PL and (R) orbito-frontal cortex contusion	Drain tract (R), hemosiderin deposits (R) PL and (R) orbito-frontal cortex	1
TBI 3 22.5/M/RH	17.6		(L) FL shearing injuries, splenium and body corpus callosum contusion	(R) FL contusion	1
TBI 4 28.1/M/RH	18.6		FL contusion, (L) FL subdural haematoma, (L) TL and (R) PL haemorrhage	Drain tract (L), FL contusion	1.5
TBI 5 17.9/F/RH	12.9	8	Contusion (location not specified in available records)	–	0
TBI 6 30.8/M/RH	24.8		(L) FL/PL contusion	FL shearing injuries periventricular white matter	1
TBI 7 34.6/M/RH	28.9		(R) amygdala and basal ganglia and (R) PL haemorrhage, (L) FL inflammatory changes	(L) TL contusion	1
TBI 8 16.8/M/RH	9.1		(L) TL and (L) FL punctiform and (R) mesencephalon contusion, (L) FL and (L) thalamus haemorrhagic injuries	Orbito-frontal cortex contusion, enlarged ventricles	1
TBI 9 33.8/M/RH	27.9	7		Drain tract (R), thalamus injury, corpus callosum shearing injuries, (R) FL and (L) inferior FL and (R) OL contusion	2.5
TBI 10 26.9/F/RH	23.9		FL injuries	Drain tract (L), PL and OL/PL and FL and (R) TL shearing injuries, slightly enlarged ventricles	1
TBI 11 28.3/F/RH	21.9		FL and (L) TL perfusion deficits	Drain tract (R), wide extended FL contusion, cerebellar atrophy	2
TBI 12 22.3/M/RH	19.1		Contusion and DAI (location not specified in available records)	(L) thalamus and (L) TL and (L) orbito-frontal cortex and (L) FL and (R) FL and central sulcus shearing injuries	2
TBI 13 31.7/M/RH	29.6	7	(L) FL/TL haemorrhage and DAI, FL and TL/OL shearing injuries	TL and (R) orbito-frontal cortex and (R) inferior FL contusion, corpus callosum degeneration, asymmetric ventricles, (L) PL shearing injury	2
TBI 14 16.7/M/RH	14.5		Enlarged (R) lateral ventricle, (R) haematoma occipital horn lateral ventricle, hyperdensity (L) thalamus and PL/TL, (LH) shearing injuries	Drain tract (R), (L) corpus callosum and thalamus and (R) PL and (L) FL and (R) TL shearing injuries, occipital horn lateral ventricle asymmetrically enlarged	2
TBI 15 28.1/M/RH	18.4		Hemosiderin deposits corpus callosum, DAI, ischaemic injury (L) occipital horn of lateral ventricle	Drain tract (R), (R) periventricular white matter FL and thalamus injuries, corpus callosum degeneration	2
TBI 16 27.9/M/RH	24.9		(L) thalamus and (L) periventricular and corpus callosum and brainstem and TL shearing injuries	Drain tract, (L) thalamus and corpus callosum and (L) TL shearing injuries	2
TBI 17 30.9/M/RH	28.3	7	Lesion and location not specified in available records	Drain tract (R), (L) inferior TL contusion, (L) anterior cingulate and (R) FL and central sulcus shearing injuries	2
TBI 18 24.1/M/RH	21.8		(L) FL haematoma, FL intraparenchymal haemorrhage, subarachnoidal bleeding	Drain tract (R), orbito-frontal cortex and (L) cerebellum contusion	2
TBI 19 19.2/M/RH	16.5		Lesion and location not specified in available records	Drain tract (R), corpus callosum degeneration, central sulcus and SMA and corpus callosum shearing injuries	2

Table 1 continued

TBI patient age/ gender	Age at injury	GCS score	Acute scan within 24 h after injury Lesion location/pathology	MRI scan at examination Lesion location/pathology	Severity score
TBI 20 26.3/M/RH	23.6		Contusion location not specified in available records	Corpus callosum and body nucleus caudatus shearing injury	2
TBI 21 20.6/F/RH	18.1	4	Diffuse axonal injuries, (L) FL/TL/PL subdural haematoma, FL contusion, injuries corpus callosum	FL and (R) PL contusion, orbito-frontal cortex shearing injuries, enlarged ventricles	2

RH right hemisphere, *LH* left hemisphere, *FL* frontal lobe, *TL* temporal lobe, *PL* parietal lobe, *OL* occipital lobe, *R* right, *L* left

Other codes: *TBI* traumatic brain injury, *MRI* magnetic resonance imaging, *RH* right-handed, *M* male, *F* female, *GCS* Glasgow coma scale score

by subtracting time to complete part A from part B. The task took less than 10 min to administer.

MRI data acquisition

Diffusion tensor images were acquired with a 3-T Magnetom Trio MRI scanner (Siemens, Erlangen Germany) using a twice refocused single shot spin echo sequence with the following parameters (Jones and Leemans 2011): slice thickness = 2.9 mm; repetition time = 7,200 ms, echo time = 81 ms, number of diffusion directions = 64, diffusion weighting = 1,000 s/mm², number of sagittal slices = 56, in-plane resolution = 2.2 × 2.2 mm² with field of view of 210 × 210 mm².

Moreover, for all subjects a high-resolution T1-weighted structural image was acquired using magnetization prepared rapid gradient echo for anatomical detail (repetition time = 2,300 ms, echo time = 2.98 ms, in-plane resolution 1 × 1 mm² with field of view of 240 × 256 mm², 160 sagittal slices with 1.1 mm thickness). These structural MRI scans were investigated by an expert neuro-radiologist to indicate location and type of pathology (e.g., shearing, haemorrhage) and identify the degree of diffuse axonal injury (Table 1).

Construction of structural networks

One structural network was generated for each subject using the subject's DTI data. In graph theory, a network is defined as a set of nodes (denoting anatomical regions) and interconnecting edges (denoting structural connections between cortical and subcortical regional nodes) (Bullmore and Sporns 2009). Because DTI tractography does not differentiate between efferent and afferent fibers, the reconstructed graphs were all undirected. We describe here some of the major steps that we went through from DTI processing to compute the topological metrics of the graph.

DTI preprocessing

The DTI data were analyzed and processed in ExploreDTI (Leemans et al. 2009), as described previously (Cae-nyenberghs et al. 2010a, b, 2011): (a) Subject motion and eddy-current induced geometrical distortions were corrected (Leemans and Jones 2009) (b) the diffusion tensors were calculated using a non-linear regression procedure (Basser and Pierpaoli 1996), and (c) DTI data were transformed to MNI space.

White matter tractography

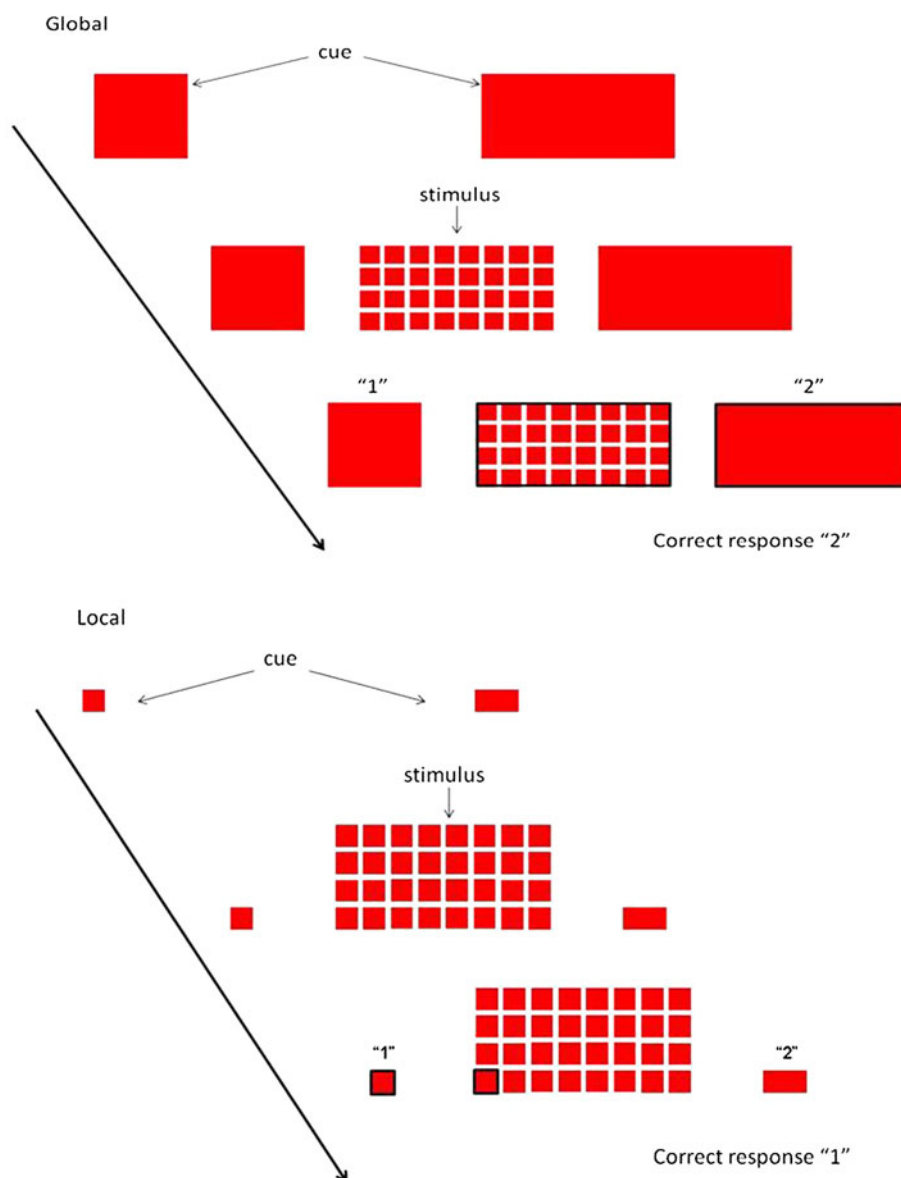
Specifically, for each individual dataset, WM tracts of the brain network were reconstructed using a deterministic streamline fiber tractography approach (Basser et al. 2000). Fiber pathways were reconstructed by defining seed points distributed uniformly throughout the data at 2 mm isotropic resolution and by following the main diffusion direction (as defined by the principal eigenvector) until the fiber tract entered a voxel with FA < 0.20 or made a high angular turn (angle >45 deg) considered to be not anatomically plausible. The step size was set at 1 mm.

Network construction

The whole-brain fiber tract reconstructions of the previous step were parcellated using the automated anatomical labeling atlas (AAL, Tzourio-Mazoyer et al. 2002). This procedure of defining the nodes has been previously described in Bassett and colleagues (2011). Using this procedure, we obtained 116 cortical and subcortical regions (58 for each hemisphere), each ROI of the AAL template representing a node of the network (see Figs. 2, 3), and the edges between each pair of nodes reflecting the corresponding reconstructed white matter tract.

Inter-regional connectivity was then examined by determining the percentage of tracts (number of fiber

Fig. 1 Local global task. Each trial started with a cue, indicating whether attention had to be paid to the global or local level. When the stimulus appeared, subjects had to rapidly decide whether the relevant level consisted of *squares* or *rectangles*



connections normalized for the total number of tracts) between any two masks (i.e. any two regions of the AAL template). This value became the edge weight in the connectivity matrix.

In the main analysis, a weighted graph approach was used. To test the role of the weighting on possible organizational differences between the brain network of patients and healthy controls, an additional test was performed in which the weighting was omitted from the analysis. For each individual dataset, all non-zero weights (i.e., all connections) were set to one and to zero otherwise (van den Heuvel et al. 2010). The end result of this procedure was an unweighted binary network. Thus, for each participant, there were two different kinds of WM networks ('percentage of tracts' and binary), each of which was represented by a symmetric 116×116 matrix.

Graph theory analysis

We investigated the properties of the structural network at the global and regional (nodal) levels using the Brain Connectivity Toolbox (Rubinov and Sporns 2010; <https://www.sites.google.com/a/brain-connectivity-toolbox.net/bct/>), quantifying the network architecture in terms of the **small-worldness, normalized clustering coefficient, normalized path length, characteristic shortest path length, clustering coefficient, strength, and global efficiency**. We described the regional properties in terms of local efficiency and betweenness centrality. Based on the constructed structural network, we looked for significant differences in global and nodal properties between the TBI children and controls. In the Supplemental Material, we only provide brief, formal definitions of each of the network properties used in this

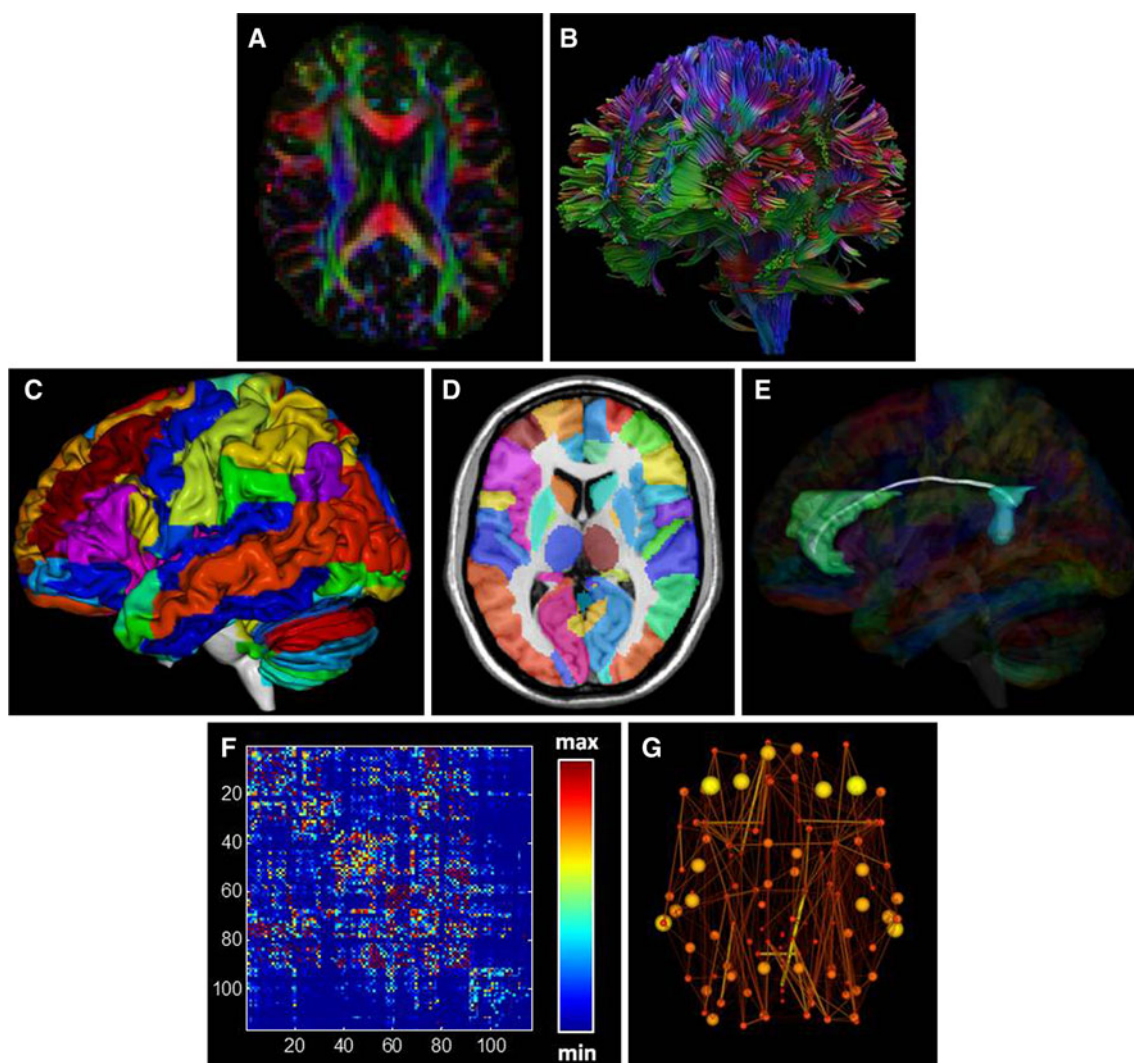


Fig. 2 Flow chart of constructing a DTI-based network. First, for each DTI dataset **a** whole brain deterministic tractography **b** was performed using ExploreDTI (see “[Materials and methods](#)”). The AAL template, consisting of 116 unique brain regions (**c–d**), was then used to segment the fiber bundles between each pair of ROIs. In **e**, an example of cortical regions and the WM fibers, linking the right

anterior cingulate gyrus with the right posterior cingulate gyrus. We next determined the percentage of tracts between each pair of regions of the AAL template, resulting in the 116×116 connectivity matrix (**f**). Next, from the resulting brain network **g** overall organizational characteristics and node-specific organizational characteristics were computed and compared between patients and healthy controls

study. For more details and in-depth discussion of these metrics, the interested reader is referred to Rubinov and Sporns (2010).

Statistical analysis

For completion times of the TMT, a 2-way ANOVA (Group \times Trail type) was performed. Trail type consisted of two levels, i.e., Trails A (Letters) and Trail B (Letters/numbers). Group contained two levels, i.e. TBI and control group. To determine the between-group differences in switch cost, a two-sample *t* test was performed. The analysis of the reaction times of the LGT were subjected to a repeated-measures ANOVA with factors Group (TBI,

controls), Cue condition (Global, Local), and Switch condition (Switch, Repeat). Significant main and interaction effects were further explored by post hoc tests using Tukey’s correction. For the switch cost and accuracy rate of the LGT, two-sample *t* tests were performed for comparing the TBI group with the age matched control group.

Statistical comparisons of all network measures (i.e. small worldness, normalized clustering coefficient, normalized path length, characteristic shortest path length, clustering coefficient, strength, global efficiency, and local efficiency) between the two groups were performed using two-sample *t* tests.

To determine whether the network organization in TBI was correlated with performance on the executive function

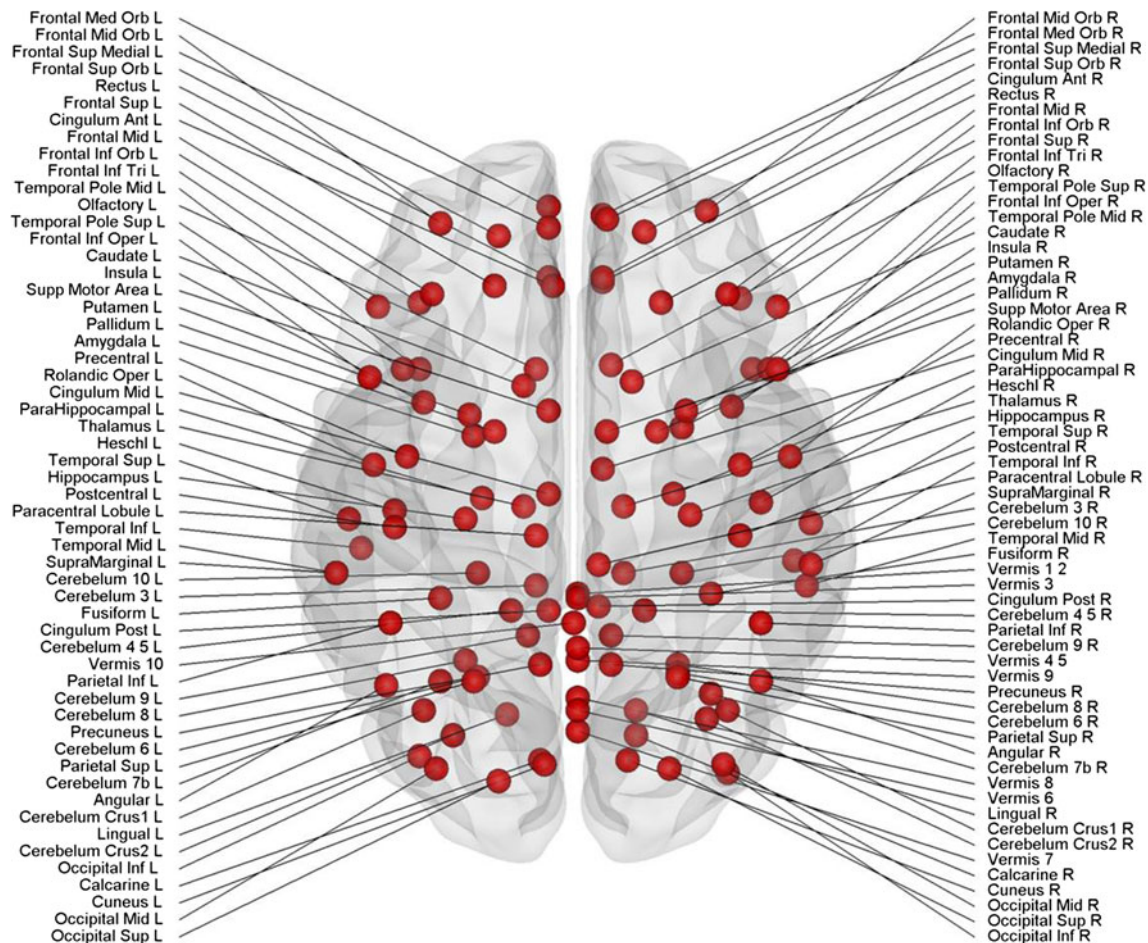


Fig. 3 Cortical and subcortical regions (58 in each hemisphere; 116 in total) as anatomically defined by a prior template image in standard stereotaxic space

tasks, we calculated Pearson's correlation coefficients of the network parameters against the behavioral parameters. Bonferroni's corrections for multiple comparisons were made, hence $p_{\text{corr}} < 0.0004$ was considered significant following correction for the node-specific analyses regarding the 116 ROIs. The grades of diffuse axonal injury were also used to assess relationships between the topological properties and severity score. To this end, we applied the Spearman's rank correlation within the TBI group. All statistical analyses were performed with the Statistica software (StatSoft, Inc).

Results

Behavioral performance

Instrumented task: local global task (LGT)

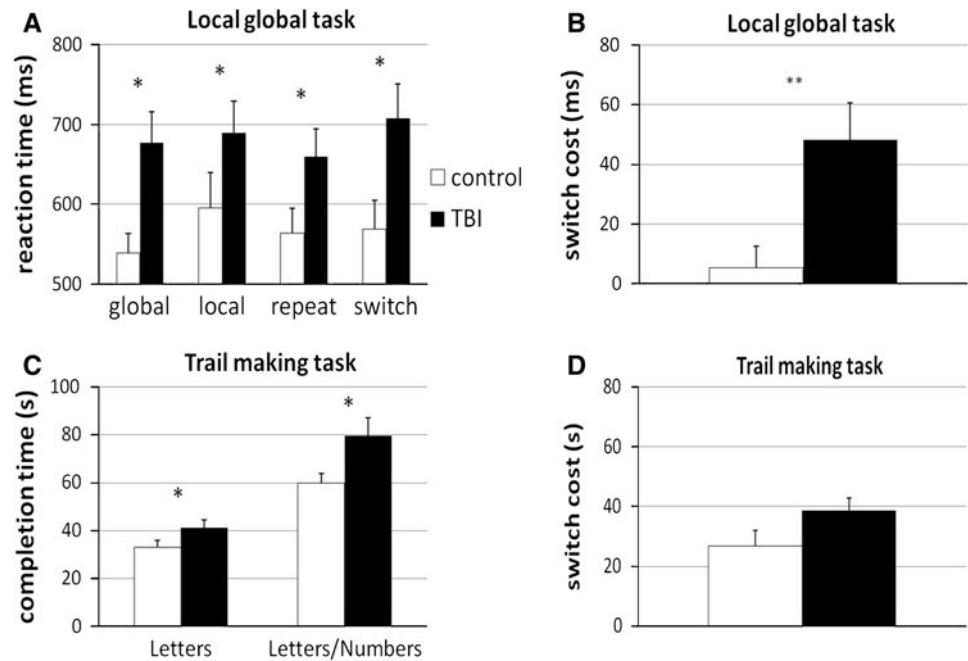
For reaction times of the local and global trials in the LGT, there were significant main effects of Cue condition

[$F(1,33) = 5.78, p < 0.05$], and Group [$F(1,33) = 4.50, p < 0.05$] (Fig. 4a). Global level information (608 ± 25 ms) was processed faster than information of local trials (642 ± 31 ms), and the controls (567 ± 40 ms) responded faster than the TBI patients (683 ± 37 ms). The interaction between the two factors was not significant.

For reaction times of the repeat and switch trials, there were significant main effects of Switch condition [$F(1,33) = 11.35, p < 0.01$], with longer reaction times for the switching trials, and Group [$F(1,33) = 4.58, p < 0.05$], with TBI patients responding more slowly compared with controls. Moreover, there was a significant interaction effect between the two factors [$F(1,33) = 7.21, p < 0.01$] (Fig. 4a). Post hoc (Tukey) testing revealed only a significant difference between the switch (708 ± 41 ms) and repeat (659 ± 34 ms) trials within the TBI group.

The mean accuracy rate (of the switch trials) and switch cost (switch reaction time–repeat reaction time) also differed significantly between the TBI patients (accuracy: mean = 92.3 %; range = 70.8–100 %, switch cost: mean = 48.2 ms; range = –33.3–197.5 ms) and the controls

Fig. 4 Behavioral task performance. **a** Reaction time of the different trial types of the local global task; **b** completion time of Trails A and B of the trail making task; **c** switch cost of the local global task; and **d** switch cost of the trail making task. TBI, black bars control, white bars ** $p < 0.01$, * $p < 0.05$ for the TBI group compared to controls; TBI, traumatic brain injury



(accuracy: mean = 97.9 %; range = 87.5–100 %; switch cost: mean = 5.4 ms; range = –48.9–58.8 ms), accuracy: $t(33) = 2.36$, $p < 0.05$, switch cost: $t(33) = -2.68$, $p < 0.01$) with the lower accuracy scores and higher switch cost in the TBI subjects indicating poorer switching performance than in the controls, as shown in Fig. 4b.

Clinical test: trail making task (TMT)

In the TMT, a 2-way ANOVA showed that controls (mean: 46.34 ± 4.61 s) performed faster than TBI patients (mean 60.54 ± 4.15 s) on all conditions, $F(1,36) = 5.24$, $p < 0.05$ (Fig. 4c). There was also a difference between Trails A (Letters, mean: 37.09 ± 2.24 s) and Trails B (Letters/Numbers, mean: 69.79 ± 4.45 s), $F(1,36) = 95.8$, $p < 0.001$. The interaction between Group and Trail type reached marginal significance, $F(1,36) = 3.09$, $p = 0.09$. Finally, values of switch cost tended to be higher in the TBI group, $t(36) = -1.76$, $p = 0.09$ (Fig. 4d).

Small world topology

Using graph theoretical analysis, we showed that the WM structural networks of both groups exhibited a much higher local interconnectivity of the nodes (normalized clustering coefficient, $\gamma \gg 1$) (TBI group: mean = 1.44, SD = 0.16; control group: mean = 1.37, SD = 0.06) and an equivalent shortest path length between any pair of nodes (normalized path length, $\lambda \approx 1$) (TBI group: mean = 0.96, SD = 0.03; control group: mean = 0.97, SD = 0.02), compared with the matched random networks. The small worldness ($\sigma = \gamma/\lambda$) calculated from these indices was also larger

than 1 (TBI group: mean = 1.51, SD = 0.20; control group: mean = 1.42, SD = 0.04). Furthermore, the overall normalized path length λ did not differ between patients and healthy controls ($p = 0.52$). We only found a marginally increased local interconnectivity ($p = 0.09$) in the structural network of the TBI patients. In summary, TBI patients displayed prominent small-world values close to the values of the brain network of healthy controls.

TBI-related alterations

Using two-sample t tests, we found that the weighted clustering coefficient and connectivity strength, showed no significant differences between the TBI and control groups (all p 's > 0.05). The absence of these group effects suggests that local connectivity is relatively intact in TBI.

However, we observed that TBI networks had increased weighted characteristic shortest path length [$t(36) = -2.64$, $p < 0.01$] in WM networks as compared to the controls. For efficiency measurements, the local and global efficiency were computed. When compared with the controls, WM networks of TBI patients showed no significant changes in the local efficiency ($p > 0.05$), but showed significantly reduced global efficiency [$t(36) = 2.95$, $p < 0.01$]. These results imply that the global organization of WM networks of TBI patients is significantly altered.

Identification of hubs

Structural network analysis estimated for TBI and controls revealed that both groups exhibit hubs. In particular, 12

hub regions were shared by both groups, such as the bilateral precuneus, bilateral superior parietal gyrus, right superior frontal gyrus, and left middle occipital gyrus. These hubs are predominantly located in the regions of the association cortices that receive convergent inputs from multiple cortical regions (Mesulam 1998). These results are consistent with those from previous studies in healthy controls (Hagmann et al. 2008; Iturria-Medina et al. 2008; Gong et al. 2009) and patient groups (Shu et al. 2009).

The bilateral thalamus, bilateral putamen, and bilateral caudate nuclei were also identified as hub regions for both groups. These regions comprised the main nuclei of the basal ganglia, associated with a variety of functions, including set shifting, switching, and stopping behaviour (Aron and Poldrack 2006; Coxon et al. 2010; Forstmann et al. 2012). Of note, two brain regions, the left superior frontal gyrus and the right insular cortex, were identified as hubs in the control group, but not in the TBI group. Two other brain regions, the left pallidum and left middle temporal gyrus, were identified as hubs in the TBI group but not in the control group.

Correlation between network parameters of the WM structural network and executive function variables in the TBI group

We next examined the relationships between the efficiency metrics and cognitive performance. We considered only the efficiency metrics as network properties in these analyses, because these measures have been suggested to be important measures in graph theory analysis (Rubinov and Sporns 2010). If any significant correlation was found between global efficiency and performance on the switching tasks, we conducted region-specific correlation analyses between nodal efficiency and behavioral performance. Bonferroni's corrections for multiple comparisons were made, hence $p_{\text{corr}} < 0.0004$ was considered significant following correction for the node-specific analyses regarding the 116 ROIs.

In the control group, none of the executive performance variables showed significant correlations with the network metrics. The following descriptions focus on the results in the TBI group.

Local global task

A significant negative correlation was found between global efficiency and switch cost of the LGT ($r = -0.50$, $p < 0.05$). In other words, a decrease in global efficiency was associated with lower switching performance (i.e., higher switch cost) in the TBI group. In nodal characteristics, we observed significant negative correlations between switch cost of the LGT and nodal efficiency

of the right hippocampus ($r = -0.76$), left postcentral gyrus ($r = -0.78$), and left cerebellar lobule Crus II ($r = -0.73$).

The reaction time of all trial types of the LGT was also significantly related to mean global network efficiency (global trials: $r = -0.60$, $p < 0.01$, local trials: $r = -0.59$, $p < 0.01$, repeat trials: $r = -0.58$, $p < 0.01$, switch trials: $r = -0.61$, $p < 0.01$). Hence, faster performance on the LGT was associated with a higher global efficiency.

Furthermore, node-specific correlation analyses showed that reaction time of the switch trials was significantly negatively correlated with the nodal efficiency of the right superior frontal gyrus ($r = -0.73$), right middle frontal gyrus ($r = -0.74$), right inferior frontal gyrus (pars opercularis: $r = -0.75$; pars triangularis: $r = -0.74$), right hippocampus ($r = -0.80$), left middle occipital gyrus ($r = -0.75$), left postcentral gyrus ($r = -0.78$), right supramarginal gyrus ($r = -0.76$), right precuneus ($r = -0.75$), and right thalamus ($r = -0.74$) (Fig. 5).

Reaction time of the repeat trials was significantly correlated with the nodal efficiency of the left middle occipital gyrus ($r = -0.74$). In addition, we found that the reaction time of the local trials was significantly negatively correlated with the nodal efficiency of the right superior frontal gyrus ($r = -0.75$), right middle frontal gyrus ($r = -0.77$), right inferior frontal gyrus (pars opercularis: $r = -0.75$), right hippocampus ($r = -0.77$), left postcentral gyrus ($r = -0.76$), right supramarginal gyrus ($r = -0.77$), right precuneus ($r = -0.74$), and right thalamus ($r = -0.74$).

Finally, there were significant negative correlations between the reaction time of the global trials and nodal efficiency of the right inferior frontal gyrus (pars triangularis: $r = -0.75$), left middle occipital gyrus ($r = -0.78$), and right hippocampus ($r = -0.78$).

There was no significant correlation between the network efficiency parameter and the accuracy score of the LGT.

Trail-making task

First, we found that the switch cost of the TMT was significantly negatively correlated with the global efficiency ($r = -0.46$, $p < 0.05$). This score was also significantly negatively correlated with the nodal efficiency of the right medial part of the superior frontal gyrus ($r = -0.73$).

Moreover, there was a significant negative correlation between global efficiency of the network and completion time of both Trails A (letters, $r = -0.64$, $p < 0.001$) and Trails B (letters/numbers, $r = -0.57$, $p < 0.01$) with higher global efficiency being related to better performance (i.e. lower completion time) on the TMT. In nodal characteristics, we found that there was a significant negative correlation between completion time of Trails A (letters)

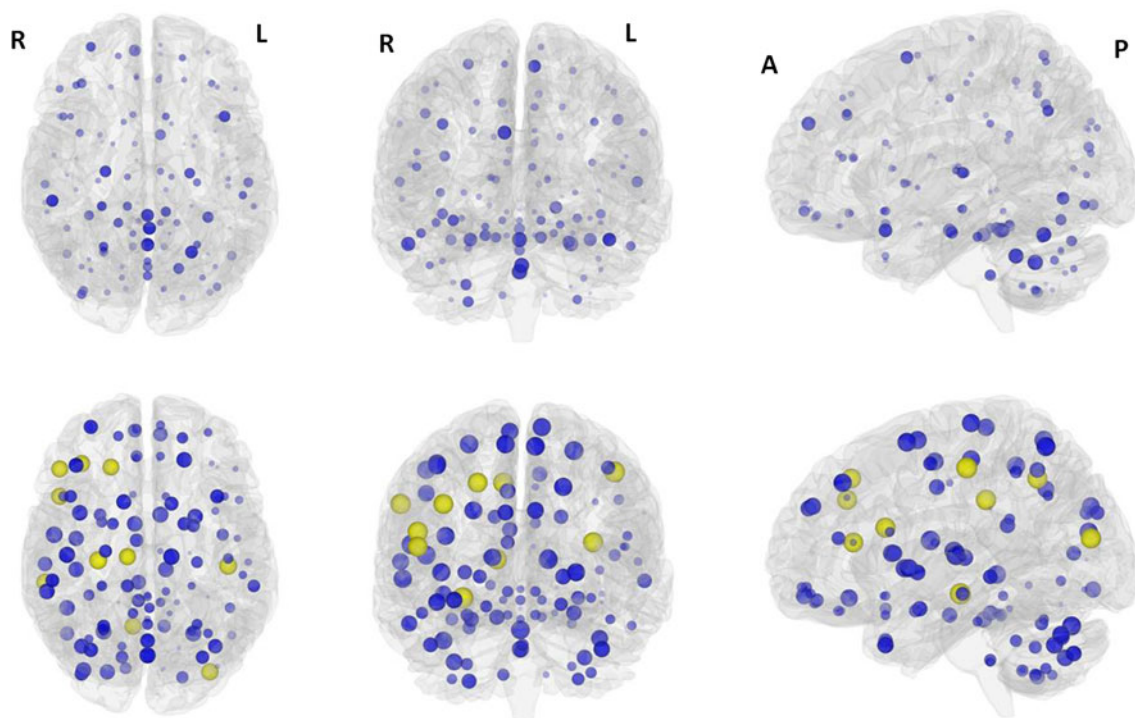


Fig. 5 Reaction time of the switch trials versus regional efficiency for the binary networks of the 116 brain regions (58 in each hemisphere). *Upper panel* controls, *lower panel* TBI patients. Size of the ROIs (spheres) represents absolute value of the correlation

coefficient. The *colors* of the nodes refer to: *yellow* significant after correction for multiple comparisons, $p < 0.0004$, *blue* not significant, $p > 0.0004$

and nodal efficiency of the right superior frontal gyrus ($r = -0.72$), left paracentral lobule ($r = -0.71$), and right supramarginal gyrus ($r = -0.74$). Secondly, completion time of Trails B (letters/numbers) was significantly negatively correlated with the nodal efficiency of the right medial part of the superior frontal gyrus ($r = -0.74$), left paracentral lobule ($r = -0.70$), and right supramarginal gyrus ($r = -0.72$).

Relationship between injury severity and network properties in the TBI patients

No significant correlations were found between injury severity and the graph metrics in the patient group or with the node-specific graph metrics even when using an exploratory uncorrected threshold ($p < 0.05$). From this, it is clear that severity score did not explain our findings.

Discussion

We investigated the white matter networks of TBI patients and healthy controls using DTI tractography and graph theoretical approaches. Both groups exhibited small-world properties in their white matter networks. However, the global efficiency was significantly decreased in the patients

when compared with controls. The decreases in efficiency were associated with poorer switching task performance. Together, our data show disrupted topological organization of white matter networks in patients with TBI, which could be responsible for the observed cognitive control deficits in these patients.

Executive control deficits in TBI patients

The behavioral results showed that the information of the easy conditions (Trails A, repeat trials, global trials) was processed faster than the information from the difficult conditions (Trails B, switch trials, local trials). This general pattern of results has been reported previously in normal subjects (Miyake et al. 2000). Here, we extend these observations to TBI patients.

In addition, controls outperformed TBI patients on all conditions of the switching tasks. This pattern extends previously reported differences in performance on executive function tasks by TBI patients (Draper and Ponsford 2008; Levin and Kraus 1994; Scheid et al. 2006) to two other tasks, one of which is commonly used for neuropsychological assessment (TMT), and the other based on the empirical constructs (local global task).

The healthy controls completed the executive control tasks more rapidly than the TBI patients. This speed

advantage was not only found for the traditionally demanding conditions, but also for the conditions not usually considered to be cognitively demanding, which are not considered to involve conflict. Although there is no inhibition required in the simpler conditions, other demands are required, such as effortful attention to complex stimuli, visual search, visual perceptual ability, monitoring, motor speed, invoking executive control. These results suggest that even simple conditions of the TMT and LGT involve some level of effortful processing for TBI patients. McAllister and colleagues (2001) have suggested that patients with TBI are less able to efficiently match available processing resources (which may be unimpaired) to the task demands. Consequently, they may over-commit processing resources to tasks without enhancing performance.

Group differences in the structural brain network

The human brain is a large, dynamic system with an optimal balance between local specialization and global integration (Bullmore and Sporns 2009). Although TBI patients showed an overall small-world topology, a significant decrease of network connectivity was found. Specifically, patients displayed a significantly increased characteristic shortest path length. The path length of a node expresses how close it is connected globally to other nodes of the network, with shorter path lengths reflecting higher levels of efficient access to information (Rubinov and Sporns 2010). The average inverse shortest path length is a related measure known as the global efficiency (Latora and Marchiori 2001), which is the most commonly used measure of functional integration (Achard and Bullmore 2007). Our TBI patients showed strong decreases in global efficiency.

Furthermore, the absence of group effects on strength and clustering coefficient marks the fact that TBI does not strongly affect the local connectivity or local organization of the brain network, indicating that the effects on global efficiency and shortest path length are likely to be related to organizational effects rather than just reduced local connectivity. In other words, our findings tend to suggest that TBI affects the global organization of the brain network. Structural networks of patients with schizophrenia also exhibited decreases in global connectivity profile, rather than effects on local organization (van den Heuvel et al. 2010). This demonstration of global topology and efficiency alteration of the brain network as a whole in TBI patients supports the notion of TBI as a ‘disconnection syndrome’ from a network perspective (Guye et al. 2010). Changes in topology have also been found in animal models of mild TBI (Patel et al. 2012). Thus, the present study complements clinical and experimental studies of TBI and emphasizes the vulnerability of the brain network as a whole.

Using functional network analyses derived from fMRI task-related data, our previous study of graph theory has demonstrated increases of ‘functional connectivity’ in TBI patients, as shown by higher values of connectivity degree and local efficiency (Caeyenberghs et al. 2012). Furthermore, the increased connectivity degree was significantly correlated with poorer switching task performance and more severe brain injury. We suggest that higher functional connectivity (i.e., a better synchronization between activity levels across neural network nodes) may be directly related to a poorer structural connectivity in TBI patients. Further studies on the association between structural and functional connectivity will be helpful to further clarify this issue.

Behavioral relevance of network alterations in TBI

In this study, significant negative correlations between executive functioning and the global efficiency of the networks were found in the TBI group. In other words, TBI patients with decreased efficiency in white matter networks displayed lower performance on the LGT and the TMT (i.e. higher switch cost, increased reaction times).

Many previous studies in TBI patients have related executive functioning to different structural and functional properties of the brain. Using voxel-based morphometry methods, Gale and colleagues (2005) revealed correlations between lower scores on cognitive tests and decreased grey matter concentration in multiple brain regions including frontal and temporal cortices, cingulate gyrus, subcortical grey matter, and the cerebellum. Moreover, our previous functional imaging study (Leunissen et al. 2012) showed that the neural circuitry supporting executive functioning (motor switching) was altered after TBI and that this altered functional engagement was related to behavioural performance across TBI patients and controls. Finally, DTI studies have shown reduced fractional anisotropy values in the whole brain and specific tracts and regions. In these studies, significant correlations between DTI metrics and cognitive functioning have been identified, such that increased WM pathology predicts greater cognitive deficits (e.g. Kraus et al. 2007; Kennedy et al. 2009; Salmond et al. 2006). Although none of these previous studies investigated the issue from the perspective of the brain network, they can nonetheless provide indirect support for our current findings.

Previously unreported, we have now shown associations between executive deficits and structural brain organization in TBI patients from a network perspective. To our knowledge, only two studies have examined the relationship between topological parameters and cognitive functioning. Li and colleagues (2009) demonstrated that higher intelligence scores corresponded to a shorter characteristic path length and a higher global efficiency of the structural

network in healthy adults. Another study reported that several cognitive domains, including processing speed, memory, language, visuospatial, and executive functions, were associated with efficiency of the structural brain network of elderly people (Wen et al. 2011). Taken together, our findings support the previous observations that cognitive control processes are dependent on the fidelity of the underlying white matter to facilitate the rapid and error-free transmission of data between different brain regions.

Node-specific correlation analyses performed within the TBI group revealed significant correlations between the switching performance test scores and the local efficiency of multiple brain regions, including cortical regions located in the parietal, occipital, temporal, and frontal lobes, as well as subcortical structures such as the thalamus, hippocampus and cerebellum.

First, performance on the LGT was significantly related to efficiency within the (dorsolateral) prefrontal regions of the structural brain network, including the middle frontal gyrus. The switching tasks in our study required flexible adjustments of behavior and adaptations to sudden changes, which are an expression of executive functioning (Gilbert and Burgess 2008). Moreover, the functional MRI activations involved in motor task switching (Coxon et al. 2010; Leunissen et al. 2012), including the dorsolateral prefrontal cortex, are consistent with our finding of a relation between improved performance on the switching tasks and higher efficiency in the prefrontal regions. Higher efficiency within the right inferior frontal cortex was also associated with shorter reaction times on the LGT. This region has a role in the attentional capture of salient stimuli (Sharp et al. 2010) and is a critical node in the inhibition network (Aron and Poldrack 2006).

Secondly, the performance on the switching tasks was also correlated with nodal efficiency of parietal regions, including the right precuneus and right supramarginal gyrus. Recent data have supported that these regions are involved in top-down attention and visuospatial processing to maintain the information in short-term memory (Behrmann et al. 2004; Cavanna and Trimble 2006; Hester et al. 2005). This is consistent with the notion that executive functions are supported by a superordinate cognitive control network, including parietal regions (Niendam et al. 2012).

Third, the correlation analyses provided evidence that deficits in switching are related to lower efficiency in the occipital, i.e. left middle occipital gyrus, and sensorimotor regions, including the right superior frontal gyrus (corresponding to the dorsal premotor cortex), right medial superior frontal gyrus (corresponding to the supplementary motor area), left paracentral lobule, and left postcentral gyrus. This is consistent with the notion that both the TMT and LGT require precise motor control based on the online processing of visual information.

Finally, performance on the switching tasks was also significantly correlated to nodal efficiency in subcortical structures, such as the left cerebellum Crus II, right hippocampus, and right thalamus. Contemporary clinical studies suggest that the posterior cerebellum contributes to complex cognitive operations (e.g., Schmahmann et al. 2007). A recent meta-analysis showed that executive tasks (such as N-back tasks or mental rotation tasks) activate regions of Crus II (Stoodley and Schmahmann 2009). Furthermore, it was found that cognitive impairments occur when posterior cerebellar lesions affect Crus II, disrupting prefrontal-cerebellar loops (Stoodley and Schmahmann 2010). The hippocampus supports not only the encoding and retrieval of certain memory representations, but also their translation into adaptive behavior (Bast 2007). The hippocampus appears to combine: (1) sensory afferents and synaptic mechanisms underlying certain types of rapid learning; and (2) links to behavioral functions, including executive functions. The thalamus is also known to gate and mediate many cognitive functions (Carrera and Bogousslavsky 2006; Sidaros et al. 2009). Moreover, thalamic lesions have been associated with a decrease in executive function with larger lesions associated with greater deficits (Kubat-Silman et al. 2002; Van der Werf et al. 2000). A previous DTI study has also found a correlation between executive function and fractional anisotropy in the thalamic nuclei (Little et al. 2010). These findings further emphasize the role of subcortical-cortical pathways in executive functioning that has previously only been ascribed to cortico-cortical circuits, such as the anterior cingulate-prefrontal loop (Ide and Li 2011).

All these node-specific results are consistent with previous findings that short paths in the brain network assure effective integrity or rapid transfer of information between and across remote regions that are believed to constitute the basis of cognitive functioning (Sporns and Zwi 2004).

Clinical relevance

The presented method of DTI in combination with the calculated network parameters could make these techniques a promising adjunctive tool to improve TBI diagnostics/prognosis and for follow-up of cognitive deficits. Future work might include efforts using graph theoretical measures to quantify how therapeutically effective treatments (i.e. cognitive training) remediate topologically suboptimal network configurations in TBI patients.

Methodological considerations and limitations

First, testing patients with TBI introduces a number of methodological factors that may affect interpretation of results: TBI is a heterogeneous disease with multiple

deficits that evolve over time. In addition, findings will likely be affected by the time of testing relative to the time of injury (as indicated in Table 1). However, the group was relatively homogeneous in terms of injury mechanism and neuropathology (DAI). Moreover, each control was carefully selected to match the patient's demographics (age).

Second, in this study, we employed a deterministic tractography approach (Basser et al. 2000; Mori et al. 1999) to define the edges of the structural network. However, it has been shown recently that there are many brain regions with complex fiber architecture, also referred to as “crossing fibers” (Jeurissen et al. 2012; Tournier et al. 2011). The tracking procedure may terminate prematurely when it reaches regions with fiber crossings as low fractional anisotropy values may be encountered (Mori and van Zijl 2002). This will result in the loss of some existing fibers, and hence some edges of the network. In this context, tractography approaches based on the more advanced diffusion models, such as diffusion spectrum magnetic resonance imaging (DSI) (Wedeen et al. 2005, 2008) or high angular resolution diffusion imaging (HARDI) with Q-ball reconstruction of multiple fiber orientations (Hess et al. 2006; Tuch 2004; Jeurissen et al. 2011) may provide more accurate anatomical connectivity patterns of brain networks for solving the fiber crossing problem.

Another limitation of tractography, especially for long distance fiber bundles, is erroneous tracking results due to noise and resolution limitations (Mori and van Zijl 2002). In addition, a deterministic tracking algorithm can typically only progress when there is a high certainty of fiber direction, limiting their usefulness in reaching parts of the brain close to the gray matter. In the future, it might be more meaningful to use probabilistic tractography algorithms, including the uncertainty of each fiber orientation in the tracking procedure and establishing the spatially distributed degree of connection confidence across the whole brain to a given start point (e.g., Behrens et al. 2007; Descoteaux et al. 2009; Jeurissen et al. 2011). These probabilistic tractography algorithms have already been successfully applied in previous graph theoretical studies in healthy adults (Gong et al. 2009; Iturria-Medina et al. 2008, 2011) and clinical populations (Li et al. 2012; Vaessen et al. 2012).

Third, percentage of tracts was used to weight the edges in the calculation of the connectivity matrices and consequently the graph metrics. Other definitions of edge weight, such as fractional anisotropy, mean diffusivity, level of myelination, and the number of fibers have previously been used (e.g., Gong et al. 2009; Hagmann et al. 2010; Vaessen et al. 2012; van den Heuvel et al. 2010). Currently, no consensus prevails which weighting factor in the construction of the graphs is the most representative measure of structural connectivity. To test the robustness of our

results, we also constructed networks weighted by fractional anisotropy and mean diffusivity values. The results of those networks were comparable with those of the presented WM networks (percentage of tracts and binary).

Finally, newer gradient echo imaging methods have further improved the detection of susceptibility-related effects of haemorrhagic shearing injury, such as susceptibility weighted imaging (SWI) (Grados et al. 2001; Tong et al. 2003, 2004). Because SWI is much more sensitive in detecting haemorrhagic DAI, more accurate data can be obtained to objectively assess the severity of injury. The extent of detected haemorrhage can provide long-term neurological and behavioral prognostic information. Further studies correlating the abnormalities seen on SWI with graph metrics need to be done to better define the neuroimaging correlates of cognitive disorders.

Conclusions

In the present study, we used diffusion tensor tractography and graph theoretical analyses to investigate TBI-related changes in the topological efficiency in white matter structural networks. We found that when compared with controls, patients with TBI had a reduced global efficiency in their brain network. Furthermore, this reduction was correlated with lower performance on the switching tasks. Thus, our results suggest a disrupted integrity in the large-scale brain systems in TBI patients and provide structural insights into the TBI connectome.

Acknowledgments This work was supported by a grant from the Research Programme of the Research Foundation—Flanders (FWO) (G.0482.010 and G.A114.11) and Grant P6/29 from the Interuniversity Attraction Poles program of the Belgian federal government. Caeyenberghs K. is funded by a postdoctoral fellowship of the Research Foundation—Flanders (FWO).

Conflict of interest There are no conflicts of interest.

References

- Achard S, Bullmore E (2007) Efficiency and cost of economical brain functional networks. *PLoS Comput Biol* 3:174–183
- Adams JH, Doyle D, Ford I, Gennarelli TA, Graham DI, McLellan DR (1989) Diffuse axonal injury in head injury: definition, diagnosis and grading. *Histopathology* 15:49–59
- Aron AR, Poldrack RA (2006) Cortical and subcortical contributions to stop signal response inhibition: role of the subthalamic nucleus. *J Neurosci* 26:2424–2433
- Axelrod BN, Fichtenberg NL, Liethen PC, Czarnota MA, Stucky K (2001) Performance characteristics of postacute traumatic brain injury patients on the WAIS-III and WMS-III. *Clinical Neuropsychologist* 15:516–520
- Basser PJ, Pierpaoli C (1996) Microstructural and physiological features of tissues elucidated by quantitative-diffusion-tensor MRI. *J MagnReson B* 111:209–219

- Basser PJ, Pajevic S, Pierpaoli C, Duda J, Aldroubi A (2000) In vivo fiber tractography using DT-MRI data. *Magn Reson Med* 44:625–632
- Bassett DS, Brown JA, Deshpande V, Carlson JM, Grafton ST (2011) Conserved and variable architecture of human white matter connectivity. *Neuroimage* 54:1262–1279
- Bast T (2007) Toward an integrative perspective on hippocampal function: from the rapid encoding of experience to adaptive behavior. *Rev Neurosci* 18:253–281
- Behrens TEJ, Berg HJ, Jbabdi S, Rushworth MFS, Woolrich MW (2007) Probabilistic diffusion tractography with multiple fibre orientations: what can we gain? *Neuroimage* 34:144–155
- Behrmann M, Geng JJ, Shomstein S (2004) Parietal cortex and attention. *Curr Opin Neurobiol* 14:212–217
- Bruns TJ, Hauser WA (2003) The epidemiology of traumatic brain injury: a review. *Epilepsia* 44:2–10
- Bullmore E, Sporns O (2009) Complex brain networks: graph theoretical analysis of structural and functional systems. *Nat Rev Neurosci* 10:186–198
- Caeyenberghs K, Leemans A, Geurts M, Taymans T, Vander LC, Smits-Engelsman BC et al (2010a) Brain-behavior relationships in young traumatic brain injury patients: fractional anisotropy measures are highly correlated with dynamic visuomotor tracking performance. *Neuropsychologia* 48:1472–1482
- Caeyenberghs K, Leemans A, Geurts M, Taymans T, Linden CV, Smits-Engelsman BC et al (2010b) Brain-behavior relationships in young traumatic brain injury patients: dTI metrics are highly correlated with postural control. *Hum Brain Mapp* 31:992–1002
- Caeyenberghs K, Leemans A, Geurts M, Linden CV, Smits-Engelsman BC, Sunaert S et al (2011) Correlations between white matter integrity and motor function in traumatic brain injury patients. *Neurorehabil Neural Repair* 25:492–502
- Caeyenberghs K, Leemans A, Heitger MH, Leunissen I, Dholander T, Sunaert S, Dupont P, Swinnen SP (2012) Graph analysis of functional brain networks for cognitive control of action in traumatic brain injury. *Brain* 135(Pt 4):1293–1307
- Carrera E, Bogousslavsky J (2006) The thalamus and behavior—Effects of anatomically distinct strokes. *Neurology* 66:1817–1823
- Cavanna AE, Trimble MR (2006) The precuneus: a review of its functional anatomy and behavioural correlates. *Brain* 129:564–583
- Coxon JP, Goble DJ, Van IA, De VJ, Wenderoth N, Swinnen SP (2010) Reduced basal ganglia function when elderly switch between coordinated movement patterns. *Cereb Cortex* 20:2368–2379
- Demakis GJ (2004) Frontal lobe damage and tests of executive processing: a meta-analysis of the category test, stroop test, and trail-making test. *J Clin Exp Neuropsychol* 26:441–450
- Descoteaux M, Deriche R, Knosche TR, Anwander A (2009) Deterministic and Probabilistic Tractography Based on Complex Fibre Orientation Distributions. *IEEE Trans Med Imaging* 28:269–286
- Draper K, Ponsford J (2008) Cognitive functioning ten years following traumatic brain injury and rehabilitation. *Neuropsychology* 22:618–625
- Forstmann BU, Keuken MC, Jahfari S, Bazin PL, Neumann J, Schäfer A, Anwander A, Turner R (2012) Cortico-subthalamic white matter tract strength predicts interindividual efficacy in stopping a motor response. *Neuroimage* 60(1):370–375
- Gale SD, Baxter L, Roundy N, Johnson SC (2005) Traumatic brain injury and grey matter concentration: a preliminary voxel based morphometry study. *J Neurol Neurosurg Psychiatry* 76:984–988
- Gilbert SJ, Burgess PW (2008) Executive function. *Curr Biol* 18:R110–R114
- Godefroy O (2003) Frontal syndrome and disorders of executive functions. *J Neurol* 250:1–6
- Gong G, He Y, Concha L, Lebel C, Gross DW, Evans AC, Beaulieu C (2009) Mapping anatomical connectivity patterns of human cerebral cortex using in vivo diffusion tensor imaging tractography. *Cereb Cortex* 19:524–536
- Gouveia PAR, Brucki SMD, Malheiros SMF, Bueno OFA (2007) Disorders in planning and strategy application in frontal lobe lesion patients. *Brain Cogn* 63:240–246
- Grados MA, Slomine BS, Gerring JP, Vasa R, Bryan N, Denckla MB (2001) Depth of lesion model in children and adolescents with moderate to severe traumatic brain injury: use of SPGR MRI to predict severity and outcome. *J Neurol Neurosurg Psychiatry* 70:350–358
- Guilmette TJ, Dabrowski J, Kennedy ML, Gnys J (1999) A comparison of nine WAIS-R short forms in individuals with mild to severe traumatic brain injury. *Assessment* 6:33–41
- Guye M, Bettus G, Bartolomei F, Cozzone PJ (2010) Graph theoretical analysis of structural and functional connectivity MRI in normal and pathological brain networks. *MAGMA* 23:409–421
- Hagmann P, Cammoun L, Gigandet X, Meuli R, Honey CJ, Wedeen VJ, Sporns O (2008) Mapping the structural core of human cerebral cortex. *PLoS Biol* 6(7):e159
- Hagmann P, Cammoun L, Gigandet X, Gerhard S, Grant PE, Wedeen V et al (2010) MR connectomics: principles and challenges. *J Neurosci Methods* 194:34–45
- Hess CP, Mukherjee P, Han ET, Xu D, Vigneron DB (2006) Q-ball reconstruction of multimodal fiber orientations using the spherical harmonic basis. *MagnReson Med* 56:104–117
- Hester R, Foxe JJ, Molholm S, Shpaner M, Garavan H (2005) Neural mechanisms involved in error processing: a comparison of errors made with and without awareness. *Neuroimage* 27:602–608
- Ide JS, Li CSR (2011) A cerebellar thalamic cortical circuit for error-related cognitive control. *Neuroimage* 54:455–464
- Iturria-Medina Y, Sotero RC, Canales-Rodriguez EJ, Aleman-Gomez Y, Melie-Garcia L (2008) Studying the human brain anatomical network via diffusion-weighted MRI and Graph Theory. *Neuroimage* 40:1064–1076
- Iturria-Medina Y, Pérez Fernández A, Morris DM, Canales-Rodríguez EJ, Haroon HA, GarcíaPentón L et al (2011) Brain hemispheric structural efficiency and interconnectivity rightward asymmetry in human and nonhuman primates. *Cereb Cortex* 21:56–67
- Jeurissen B, Leemans A, Jones DK, Tournier JD, Sijbers J (2011) Probabilistic Fiber Tracking Using the Residual Bootstrap with Constrained Spherical Deconvolution. *Hum Brain Mapp* 32:461–479
- Jeurissen B, Leemans A, Tournier JD, Jones DK, Sijbers J (2012) Investigating the prevalence of complex fiber configurations in white matter tissue with diffusion magnetic resonance imaging. *Hum Brain Mapp*. doi:10.1002/hbm.22099
- Jones DK, Leemans A (2011) Diffusion tensorimaging. *Methods MolBiol* 711:127–144
- Kennedy MR, Wozniak JR, Muetzel RL, Mueller BA, Chiou HH, Pantekoek K et al (2009) White matter and neurocognitive changes in adults with chronic traumatic brain injury. *J IntNeuropsycholSoc* 15:130–136
- Kinnunen KM, Greenwood R, Powell JH, Leech R, Hawkins PC, Bonnelle V et al (2011) White matter damage and cognitive impairment after traumatic brain injury. *Brain* 134:449–463
- Kraus JF, McArthur DL (1996) Epidemiologic aspects of brain injury. *NeurolClin* 14:435–450
- Kraus MF, Susmaras T, Caughlin BP, Walker CJ, Sweeney JA, Little DM (2007) White matter integrity and cognition in chronic

- traumatic brain injury: a diffusion tensor imaging study. *Brain* 130:2508–2519
- Kubat-Silman AK, Dagenbach D, Absher JR (2002) Patterns of impaired verbal, spatial, and object working memory after thalamic lesions. *Brain Cogn* 50:178–193
- Latora V, Marchiori M (2001) Efficient behavior of small-world networks. *Phys Rev Lett* 87:198701
- Leemans A, Jones DK (2009) The B-matrix must be rotated when correcting for subject motion in DTI data. *MagnReson Med* 61:1336–1349
- Leemans A, Jeurissen B, Sijbers J, Jones DK (2009) ExploreDTI: a graphical toolbox for processing, analyzing, and visualizing diffusion MR data. In: 17th Annual Meeting of the International Society for Magnetic Resonance in Medicine, p 3537, Hawaii, USA
- Leunissen I, Coxon JP, Geurts M, Caeyenberghs K, Michiels K, Sunaert S et al (2012) Disturbed cortico-subcortical interactions during motor task switching in traumatic brain injury. *Hum Brain Mapp*. doi:10.1002/hbm.21508
- Levin HS (2003) Neuroplasticity following non-penetrating traumatic brain injury. *Brain Inj* 17:665–674
- Levin H, Kraus MF (1994) The frontal lobes and traumatic brain injury. *J Neuropsychiatry ClinNeurosci* 6:443–454
- Li YH, Liu Y, Li J, Qin W, Li KC, Yu CS et al (2009) Brain Anatomical Network and Intelligence. *PLoSComputBiol* 5:e1000395
- Li Y, Liu B, Hou B, Qin W, Wang D, Yu C, Jiang T (2012) Less efficient information transfer in Cys-Allele carriers of DISC1: a brain network study based on diffusion MRI. *Cereb Cortex* 22
- Little DM, Kraus MF, Joseph J, Geary EK, Susmaras T, Zhou XJ et al (2010) Thalamic integrity underlies executive dysfunction in traumatic brain injury. *Neurology* 74:558–564
- Maas AIR, Stocchetti N, Bullock R (2008) Moderate and severe traumatic brain injury in adults. *Lancet Neurology* 7:728–741
- McAllister TW, Sparling MB, Flashman LA, Guerin SJ, Mamourian AC, Saykin AJ (2001) Differential working memory load effects after mild traumatic brain injury. *Neuroimage* 14:1004–1012
- Mesulam MM (1998) From sensation to cognition. *Brain* 121:1013–1052
- Miyake A, Friedman NP, Emerson MJ, Witzki AH, Howerter A, Wager TD (2000) The unity and diversity of executive functions and their contributions to complex “frontal lobe” tasks: a latent variable analysis. *Cogn Psychol* 41:49–100
- Mori S, van Zijl PC (2002) Fiber tracking: principles and strategies - a technical review. *NMR Biomed* 15:468–480
- Mori S, Crain BJ, Chacko VP, van Zijl PC (1999) Three-dimensional tracking of axonal projections in the brain by magnetic resonance imaging. *Ann Neurol* 45:265–269
- Navon D (1977) Forest before Trees-Precedence of global features in Visual-Perception. *Cogn Psychol* 9:353–383
- Niendam TA, Laird AR, Ray KL, Dean YM, Glahn DC, Carter CS (2012) Meta-analytic evidence for a superordinate cognitive control network subserving diverse executive functions. *Cogn Affect Behav Neurosci* 12(2):241–268
- Niogi SN, Mukherjee P, Ghajar J, Johnson C, Kolster RA, Sarkar R et al (2008a) Extent of microstructural white matter injury in postconcussive syndrome correlates with impaired cognitive reaction time: a 3T diffusion tensor imaging study of mild traumatic brain injury. *Am J Neurorad* 29:967–973
- Niogi SN, Mukherjee P, Ghajar J, Johnson CE, Kolster R, Lee H et al (2008b) Structural dissociation of attentional control and memory in adults with and without mild traumatic brain injury. *Brain* 131:3209–3221
- Oldfield RC (1971) The assessment and analysis of handedness: the Edinburgh inventory. *Neuropsychologia* 9:97–113
- Patel TP, Ventre SC, Meaney DF (2012) Dynamic changes in neural circuit topology following mild mechanical injury in vitro. *Ann Biomed Eng* 40:23–36
- Rubinov M, Sporns O (2010) Complex network measures of brain connectivity: uses and interpretations. *Neuroimage* 52:1059–1069
- Salmond CH, Menon DK, Chatfield DA, Williams GB, Pena A, Sahakian BJ et al (2006) Diffusion tensor imaging in chronic head injury survivors: correlations with learning and memory indices. *Neuroimage* 29:117–124
- Scheid R, Walther KR, Guthke T, Preul C, von Cramon DY (2006) Cognitive sequelae of diffuse axonal injury. *Arch Neurol* 63:418–424
- Schmahmann JD, Weilburg JB, Sherman JC (2007) The neuropsychiatry of the cerebellum-insights from the clinic. *Cerebellum* 6:254–267
- Sharp DJ, Bonnelle V, De Boissezon X, Beckmann CF, James SG, Patel MC et al (2010) Distinct frontal systems for response inhibition, attentional capture, and error processing. *Proc Natl Acad Sci USA* 107:6106–6111
- Shu N, Liu Y, Li J, Li YH, Yu CS, Jiang TZ (2009) Altered anatomical network in early blindness revealed by diffusion tensor tractography. *PLoS ONE* 4:e7228
- Sidaros A, Skimminge A, Liptrot MG, Sidaros K, Engberg AW, Herning M et al (2009) Long-term global and regional brain volume changes following severe traumatic brain injury: a longitudinal study with clinical correlates. *Neuroimage* 44:1–8
- Sosin DM, Sniezek JE, Thurman DJ (1996) Incidence of mild and moderate brain injury in the United States, 1991. *Brain Inj* 10:47–54
- Sporns O, Zwi JD (2004) The small world of the cerebral cortex. *Neuroinformatics* 2:145–162
- Stoodley CJ, Schmahmann JD (2009) Functional topography in the human cerebellum: a meta-analysis of neuroimaging studies. *Neuroimage* 44:489–501
- Stoodley CJ, Schmahmann JD (2010) Evidence for topographic organization in the cerebellum of motor control versus cognitive and affective processing. *Cortex* 46:831–844
- Stuss DT, Bisschop SM, Alexander MP, Levine B, Katz D, Izukawa D (2001) The trail making test: a study in focal lesion patients. *Psychol Assess* 13:230–239
- Tagliaferri F, Compagnone C, Korsic M, Servadei F, Kraus J (2006) A systematic review of brain injury epidemiology in Europe. *Acta Neurochir* 148:255–268
- Teasdale G, Jennett B (1974) Assessment of coma and impaired consciousness. A practical scale. *Lancet* 2:81–84
- Thurman DJ, Alverson C, Dunn KA, Guerrero J, Sniezek JE (1999) Traumatic brain injury in the United States: a public health perspective (Review). *J Head Trauma Rehabil* 14:602–615
- Timmons SD (2012) An update on traumatic brain injuries. *J NeurosurgSci* 56:191–202
- Tong KA, Ashwal S, Holshouser BA, Shutter LA, Herigault G, Haacke EM et al (2003) Hemorrhagic shearing lesions in children and adolescents with posttraumatic diffuse axonal injury: improved detection and initial results. *Radiology* 227:332–339
- Tong KA, Ashwal S, Holshouser BA, Nickerson JP, Wall CJ, Shutter LA et al (2004) Diffuse axonal injury in children: clinical correlation with hemorrhagic lesions. *Ann Neurol* 56:36–50
- Tournier JD, Mori S, Leemans A (2011) Diffusion Tensor Imaging and Beyond. *MagnReson Med* 65:1532–1556
- Tuch DS (2004) Q-ball imaging. *MagnReson Med* 52:1358–1372
- Tzourio-Mazoyer N, Landeau B, Papathanassiou D, Crivello F, Etard O, Delcroix N et al (2002) Automated anatomical labeling of activations in SPM using a macroscopic anatomical parcellation of the MNI MRI single-subject brain. *Neuroimage* 15:273–289

- Vaessen MJ, Jansen JF, Vlooswijk MC, Hofman PA, Majoie HJ, Aldenkamp AP, Backes WH (2012) White matter network abnormalities are associated with cognitive decline in chronic epilepsy. *Cereb Cortex* 22:2139–2147
- van den Heuvel MP, Mandl RC, Stam CJ, Kahn RS, Hulshoff Pol HE (2010) Aberrant frontal and temporal complex network structure in schizophrenia: a graph theoretical analysis. *J Neurosci* 30:15915–15926
- Van der Werf YD, Witter MP, Uylings HBM, Jolles J (2000) Neuropsychology of infarctions in the thalamus: a review. *Neuropsychologia* 38:613–627
- Wedeen VJ, Hagmann P, Tseng WY, Reese TG, Weisskoff RM (2005) Mapping complex tissue architecture with diffusion spectrum magnetic resonance imaging. *MagnReson Med* 54:1377–1386
- Wedeen VJ, Wang RP, Schmahmann JD, Benner T, Tseng WY, Dai G, Pandya DN, Hagmann P, D’Arceuil H, de Crespigny AJ (2008) Diffusion spectrum magnetic resonance imaging (DSI) tractography of crossing fibers. *Neuroimage* 41:1267–1277
- Wen W, Zhu W, He Y, Kochan NA, Reppermund S, Slavin MJ et al (2011) Discrete neuroanatomical networks are associated with specific cognitive abilities in old age. *J Neurosci* 31:1204–1212